Desalination and Water Treatment
www.deswater.com
29 (2011) 29–38
May
1944-3994 / 1944-3986 © 2011 Desalination Publications. All rights reserved.
doi: 10.5004/dwt.2011.1813

Removal of hazardous dye from synthetic textile dyeing and printing effluents by *Archis hypogaea L.* shell: a low cost agro waste material

G.H. Sonawane[a], V.S. Shrivastava[b]*

[a]*Department of Chemistry, Kisan Arts, Commerce and Science College, Parola, Dist. Jalgaon - 425111 (M.S.), India*
[b]*Department of P.G. Studies and Research in Chemistry, G.T.P. College, Nandurbar - 425412 (M.S.), India*
Tel. +91 2564 234248; email: drvinod_shrivastava@yahoo.com

Received 24 January 2010; Accepted in revised form 26 October 2010

ABSTRACT

The sorption of Safranine onto the *Archis hypogaea L.* (groundnut) shell (GNS) has been studied in terms of pseudo first order, pseudo second order, Elovich and intraparticle diffusion chemical sorption processes. The batch sorption model, based on the assumption of a pseudo second order mechanism has been used to predict the rate constant of sorption and the equilibrium capacity with the effect of mass of adsorbent, initial dye concentration, pH and contact time. The rates of sorption were found to be conforming pseudo second order kinetics with good correlation. Batch isotherm studies for sorption of Safranine on *Archis hypogaea L.* shell (GNS) were described by Freundlich and Langmuir isotherm equation. In adsorption isotherms, Langmuir isotherm fits well with experimental data having $r^2 > 0.9956$. The maximum adsorption capacity observed was 172.14 mg/g. The values of dimensionless separation factor R_L are $0 < R_L < 1$ indicating that favorable adsorption. The adsorbent was also characterized by FTIR, XRD and SEM analysis.

Keywords: Adsorption kinetics; Dye removal; Safranine; *Archis hypogaea*; Isotherm; Biosorption

1. Introduction

The increasing use of organic compounds endangering the environment encourages the search for better and more efficient sorbents to remove such contaminants from water. Environmental pollution and health concerns associated with synthetic dye effluents are well recognized. Regulatory bodies to reduce the quantity of colour in effluents and water resources are enforcing increasingly stringent colour consent standards. With the growing emphasis on environment friendly industries, it is important to discover cheap and efficient methods for cleaning industrial wastewater. Various techniques for dye removal have been reported and the advantages and disadvantages have been extensively reviewed [1,2].

Adsorption has been found to be an efficient and economic process to remove dyes, pigments and other colorants. It is also used to control the biochemical oxygen demand. Activated carbon has widely been used for the removal of inorganic and organic pollutants from aqueous solutions. Activated carbon has high adsorption capacities and amphoteric properties, which enable adsorption of both cationic and anionic dyes. However, the cost of production and regeneration of activated carbon is high and its use is impractical for most pollution control applications [3]. At this juncture, use of other secondary resource materials becomes highly relevant. Numbers of low cost, easily available materials are being studied for the removal of different dyes from aqueous solutions at

* Corresponding author.

different operating conditions with different dye adsorption capacities (Table 1).

The removal of dyes from industrial wastewater is currently of great importance. Adsorption has been used extensively in industrial processes for separation and purification. Different adsorbents have been used for removal of dyes. These investigated adsorbents include chitin [4], sepiolite [5], fly ash [6] , orange peel [7], rice husk [8], apple pomace, wheat straw [9], treated saw dust, timber industry waste, cotton plant [10], palm fruit bunch particles [11], natural phosphates[12], shale oil ash [13] spent brewery grains [14] and neem leaf [15]. In the present study, the shells of groundnut (GNS) i.e. *Archis hypogaea L.* have been used as an adsorbent for the removal of Safranine from aqueous solutions. Safranine is selected as a model compound to evaluate the capability of GNS to remove dye from wastewaters in order to evaluate the adsorption capacity of GNS, contact time, pH, particle size, adsorbent doses, initial dye concentration, kinetics and isotherm studies were conducted.

2. Materials and methods

2.1. Adsorbent material

Shells of groundnut (*Archis hypogaea L.*) (GNS) were obtained nearby agricultural field, the collected shells were washed with double distilled water to remove adhering dirt and then were dried in sunlight, crushed and sieved through 60–250 μ size. These ground material was soaked in water for 18 h and washed with hot and cold distilled water, till the wash water is colorless. This washed material was then dried in oven at 50°C for 12 h and preserved in glass bottle for use as an adsorbent without any pretreatment.

2.2. Adsorbate

Safranine is a basic red dyestuff (C.I. = 50240, chemical formula $C_{20}H_{19}N_4Cl$, F.W. = 350.5, nature = basic dye λ_{max} = 532 nm) was supplied by S.D. Fine Chemicals, Mumbai used in the study. An accurately weighed quantity of dye was dissolved in double distilled water to prepare stock solution (2000 mg/l).

2.3. Experimental methods and measurement

The adsorption experiments were carried out in a batch process at constant temperature of 30°C by using aqueous solution of safranine. In each experiment an accurately weighed amount of GNS was added to 50 ml of the dye solution in 100 ml stoppard bottles and mixture was agitated on a mechanical shaker for a given time at constant temperature of 30°C. The adsorbent was separated from solution by centrifugation. The absorbance of the supernant solution was estimated to determine the residual dye concentration. The residual dye concentration was determined at 532 nm with UV-visible spectrophotometer (Systronics-2203). The experiments were carried out at initial pH values ranging from 2 to 11; initial pH was controlled by addition of 0.1 N HCl and 0.1 N NaOH solutions. Kinetics of adsorption was determined by analyzing adsorptive uptake of dye from aqueous solution at different time intervals. The effect of adsorbent dosage on percent removal was studied by varying with GNS dosage from 1 to 12 g/L, maintaining the dye concentration at 100, 200, 300 and 400 mg/L. The effect of dye concentration from 200 to 400 mg/L at an initial pH of 8 was studied. Langmuir and Freundlich isotherms were obtained from dye concentration 100–400 mg/l and varying GNS dose from 1 to 12 g/l at pH = 8 and contact

Table 1
Comparison of the monolayer capacities of various adsorbents for some dyes

Adsorbate (dye)	Adsorbent	Maximum adsorption capacity (mg/g)	Reference
Brilliant green	Bagasseflyash	65.78	6
Methylene blue	Sepiolite	2.35	1
Methylene violet	Sepiolite	2.33	1
Brilliant green	Neem leaf powder	133.69	15
Methylene blue	Neem leaf powder	19.61	15
Methyl orange	Banana, orange peel	21.0, 20.5	7
Methylene blue	Banana, orange peel	20.8, 18.6	7
Rhodamine B	Banana, orange peel	20.6, 14.6	7
Congo red	Banana, orange peel	18.2, 14.0	7
Methyl violet	Banana, orange peel	12.2, 11.5	7
Amino black	Banana, orange peel	6.5, 7.9	7
Safranine	*Archis hypogaea*	172.14	This work

time 40 min. The FTIR, XRD, SEM and EDX elements analysis of adsorbent was also carried out.

3. Results and discussion

3.1. Adsorbent characterization

For structural and morphological characteristics FTIR, XRD, SEM and EDX of GNS were carried out.

3.1.1. SEM and XRD analysis

As it is known, SEM (scanning electron microscopy) is one of the most widely used surface diagnostic tools. The SEM micrographs of GNS and GNS dyed by Safranine are shown in Fig. 1. GNS has heterogeneous surface and micro pores as seen from its SEM micrographs. The XRD pattern of adsorbent GNS showed typical spectrum at 2θ of 22° and 22.8°, respectively.

3.1.2. FTIR and elemental analysis

The FTIR measurements of GNS showed the presence of peaks for large number of functional groups viz., 3845.8, 3755.1 free –OH group, 2922.0 alkyl C–H stretching, 2852.5 –C–CH3 stretching, 2374.2 –OH stretching, 2275.8 –C–N, 1884.3–C–Cl, 1749.3 –C–OR stretching, 1556.4 > C = C < 1465.8 C–H bending of methylene group, 1037.6 –CHOH and 449.4 cm^{-1} O–Si–O bending. It is clear that the adsorbent displays a number of adsorption peaks, reflecting the complex nature of adsorbent (Table 2). The FTIR spectrum of dye adsorbed GNS shows peaks at 3647.3, 3435.8 –OH stretch, 2920 CH stretch, 2763 –C–CH_3 stretch, 2349 N–H stretch, 1747 –C–OR stretching and 1032 cm^{-1} C–O stretch. This indicates shifting of peaks of 3845.8–3647.3, 3755.1–3435.8, 2922.0 of alkyl C–H stretching shifted to 2920, and 2852.5 –C–CH_3 stretching shifted to 2763, 2374.2 –OH stretching shifted to 2349, 1749.3 –C–OR shifted to 1747 and 1037.6 shifted to 1032 cm^{-1}. The shifting of these peaks in the sample to lower frequency

Table 2
Comparison of FTIR peaks of GNS before and after adsorption of Safranine

FTIR frequency (cm^{-1})		
Before adsorption		After adsorption
3845.8	Free –OH group	3647.3
3755.1		3435.8
2900.0	alkyl –C–H stretching	2920
2852.5	–C–CH3 stretching	2763
2374.2	–OH stretching	2349
2275.8	–C≡N	
1884.3	–C–Cl	
1749.3	–C–OR stretching	1747
1556.4	>C = C<	
1465.8	C–H bending of methylene group	
1037.6	–CH–OH	1032
449.4	O–Si–O bending	

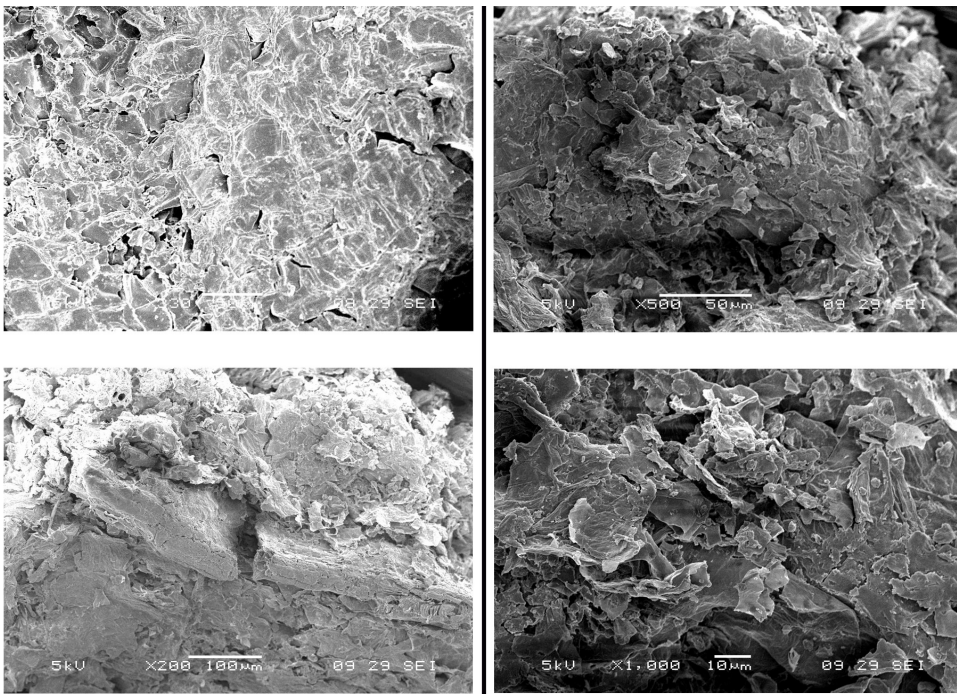

Fig. 1. The SEM micrographs of GNS and GNS dyed by Safranine.

after adsorption, suggesting the participation of these functional groups in the adsorption of Safranine by GNS.

The EDX analysis of GNS (Fig. 2) shows the presence of 42.31% C, 40.75% O and mineral composition 0.42% Na, 0.39% Mg, 1.85% Al, 2.97% Si, 7.84% K and 3.88% Ca elements.

3.2. Effect of pH

The pH of the solution affects the surface charges of adsorbent as well as the degree of ionization of different pollutants. The hydrogen ions and hydroxyl ions are adsorbed quite strongly and therefore the adsorption of other ions is affected by the pH of the solution. Change of pH affects adsorptive process through dissociation of functional groups on the adsorbent surface active sites. This subsequently leads to shift in reaction kinetics and equilibrium characteristics of adsorption process.

The adsorption of Safranine on GNS was studied in the pH range of 2–11 using 200 mg/l of dye, 4 g/l of adsorbent dose and for 40 min contact time (Fig. 3). It has been observed that the percentage of removal of Safranine increases with the increase in pH up to 8. When pH was increased from 2 to 4, the percentage of removal increased from 84.6 to 89.8%. When pH was increased to 8, percentage of removal was 91.3% and then after the gradual increase up to pH 11, it decreased to 89.3%. Hence significant adsorption of Safranine on GNS was observed at pH 8.

Two possible mechanism of adsorption of dye on the adsorbent may be considered (a) an electrostatic interaction between the adsorbent and dye molecule (b) a chemical reaction between dye and adsorbent. At acidic pH the H^+ ion concentration in the system increased and the surface of the adsorbent acquires positive charge by adsorbing H^+ ions. The lower adsorptions of dye molecule at acidic pH indicate that at low pH surface is positively charged an electrostatic repletion exists between the surface of adsorbent and cationic dye molecule leading to minimum dye adsorption. As pH of the system increases, the number of negatively charged sites increases and the number of positively charged sites decreases. Negatively charged surface sites on the GNS favor the adsorption of dye cations to the electrostatic attraction. Also higher adsorption of safranine at alkaline pH is due to presence of excess of OH^- ions which stabilize cationic dye and compete with the dye cations for the adsorption of sites.

3.3. Effect of contact time and dye concentration

To determine the equilibrium concentration and contact time, the adsorption of cationic dye Safranine on GNS was studied in relation to the function of contact time. The contact time between adsorbate and the adsorbent is of significant importance in the wastewater treatment by adsorption. A rapid uptake of adsorbate and establishment of equilibrium in a short period signifies that adsorbent can be used for its use in wastewater treatment.

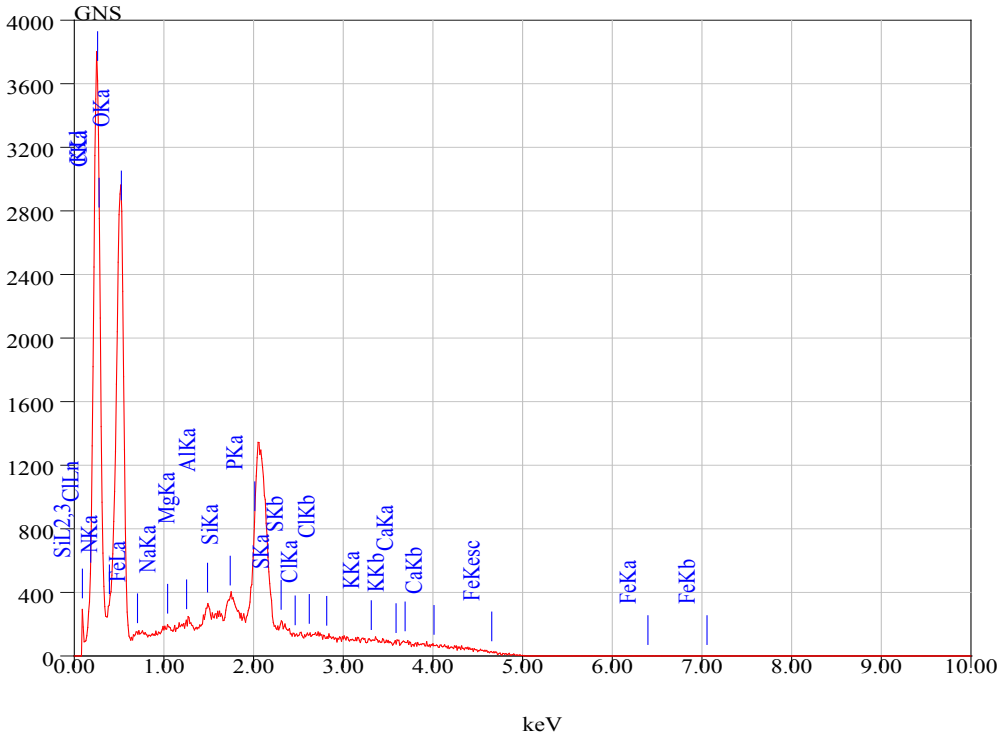

Fig. 2. The EDX spectra of GNS adsorbent.

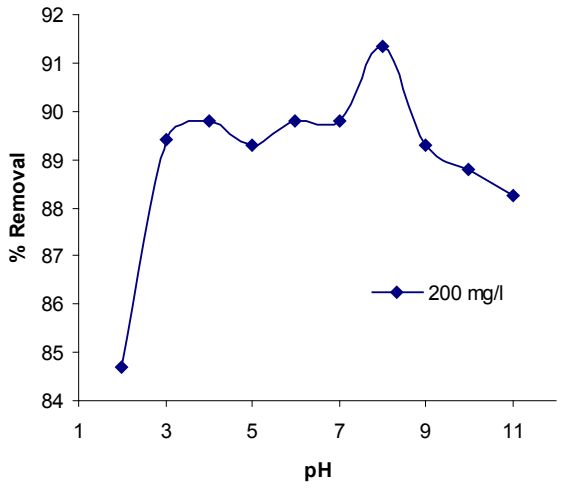

Fig. 3. Effect of pH on percent removal of safranine, initial dye concentrations 200 mg/l; adsorbent dose 4 g/l, contact time 40 min.

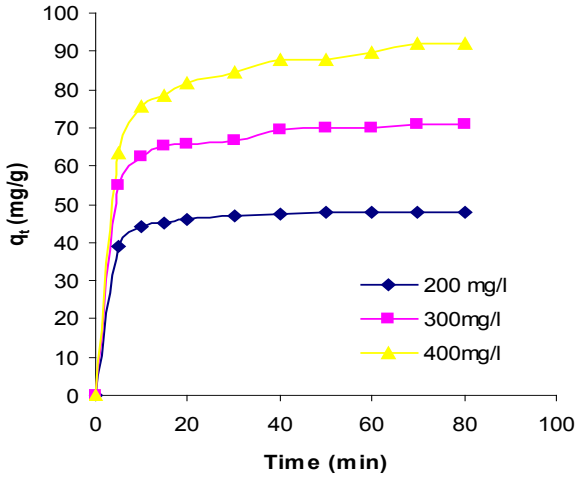

Fig. 4. Amount of dye adsorbed q_t (mg/g) with time (min) for different initial dye concentrations; adsorbent dose 4 g/l, pH 8.

In physical adsorption most of the adsorbate species are adsorbed in a short contact time. However, the strong chemical binding of the adsorbate and adsorbent requires a longer contact time for the attainment of equilibrium.

The effect of contact time on adsorption of Safranine by GNS was studied for 80 min. Initial dye concentrations 200–400 mg/l were used at 30°C and pH 8. GNS dosages used were 2–6 g/l. The contact time curve (Fig. 4) shows that the dye removal was rapid in the first 15 min. The curves of contact time are single, smooth and continuous, leading to saturation. These curves indicate the possible monolayer coverage of Safranine on the surface of GNS [16–18]. The equilibrium was attended at contact time of 40 min. When initial dye concentrations were increased from 200 to 400 mg/l for 4 g/l of adsorbent dose, the amount of dye adsorbed per unit mass of adsorbent increased from 47.5 to 87.7 mg dye/g of adsorbent (Fig. 4). From this data it is clear that the efficiency of dye removal depends on the initial dye concentration. The amount of dye adsorbed increases with increase in dye concentration and remains nearly constant after the equilibrium time.

3.4. Effect of adsorbent dosage

Adsorbent dosage is an important parameter because it determines the capacity of an adsorbent for a given initial concentration of the adsorbate. The effect of adsorbent dosage was studied on dye removal keeping all other experimental conditions constant. The percentage removal of Safranine by GNS at different adsorbent doses (1–12 g/l) for the 100–400 mg/l of dye concentrations was studied. The results shows that as the adsorbent mass increases, the overall percentage of dye adsorbed also increases but the amount adsorbed per unit mass of the adsorbent decreases considerably (Fig. 5). The decrease in

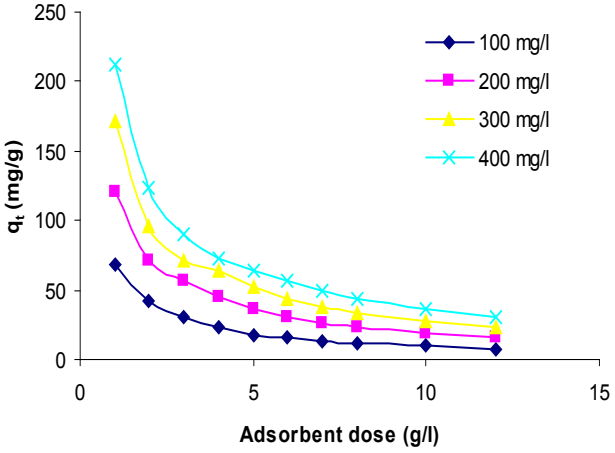

Fig. 5. Amount of dye adsorbed q_t (mg/g) with adsorbent dose (g/l) for different initial dye concentrations, contact time 40 min, pH 8.

unit adsorption with increase in the dose of adsorbent is basically due to adsorption sties remaining unsaturated during adsorption process [5]. The amount of adsorbent dose was increased from 1 to 12 g/l for 100–400 mg/l of dye concentration, 40 min contact time and pH 8 (Fig. 5), the percent removal increases from 53 to 93.1%.

3.5. Adsorption kinetics

It is important to be able to predict the rate at which contamination is removed from aqueous solutions in order to design an adsorption treatment plant. As seen from Figs. 4 and 5, the adsorption processes are quite rapid and most of the dye was retained within first 40 min contact time. In order to investigate the adsorption process of

Safranine on GNS four kinetic models were used, including pseudo-first-order, pseudo-second order, Elovich equation and intra-particle diffusion models.

3.5.1. Pseudo first order model

The pseudo first order kinetic model is more suitable for lower concentrations of solute. A linear form of pseudo first order model was described by Lagergren [19].

$$\log(q_e - q_t) = \log q_e - \frac{K_1 t}{2.303} \quad (1)$$

where q_e and q_t are the amount of dye adsorbed per unit mass of adsorbent (mg g^{-1}) at equilibrium and at time t respectively. K_1 is pseudo first order rate constant of pseudo-first order adsorption (min^{-1}). A linear plot of log ($q_e - q_t$) vs. t verifies the first order kinetics with slope yielding the value of the rate constant. The linear relationship of the plot of 200, 300, 400 mg/l dye concentration indicates the validity of equation. The first order rate constants evaluated from these plots were between 3.661×10^{-2}–8.958×10^{-2} min^{-1} for 2 g/l, 7.599×10^{-2}–9.557×10^{-2} min^{-1} for 4 g/l and 6.816×10^{-2}–10.985×10^{-2} min^{-1} for 6 g/l of adsorbent. The calculated K_1 and the corresponding linear regression coefficient r^2 values are shown in Table 3. Even though correlation coefficient r^2 for the plots are > 0.9046, the calculated q_e values from first order kinetic plots were too small as compared to the experimental q_e values (Table 3). This shows non-applicability of the pseudo-first order model in predicting kinetics of Safranine adsorption onto GNS.

3.5.2. Pseudo second order model

The rate of pseudo second order reaction is dependent on the amount of solute adsorbed on the surface of adsorbent and the amount adsorbed at equilibrium. The Ho's pseudo second order model can be represented as [20].

$$\frac{t}{q_t} = \frac{1}{K_2 q_e^2} + \frac{t}{q_e} \quad \text{and} \quad h = K_2 q_e^2 \quad (2)$$

where K_2 is the rate constant of second order adsorption (g mg^{-1} min^{-1}) and h is the initial dye adsorption rate (mg/g min). The plot of t/q_t vs. t of the above equation gives linear relationship (Fig. 6), from which q_e and K_2 can be determined from slope and intercept of the plot respectively. The linear plot of t/q_t vs. t shows a good agreement of experimental data with the second order kinetic model for different initial dye concentrations of

Table 3
Comparison of adsorption rate constants, calculated and experimental q_e values for different initial dye concentrations and adsorbent dose for different kinetic models for GNS Safranine

Adsorbent (g/l)	Dye concentration (mg/l)	Pseudo first order			
		q_e (exp) (mg/g)	$K_1 \times10^{-2}$ (min^{-1})	q_e (cal) (mg/g)	r^2
2	200	84.69	8.958	38.212	0.9955
	300	115.31	4.951	51.333	0.9699
	400	146.94	3.661	58.708	0.9046
4	200	47.70	9.557	11.904	0.9855
	300	69.90	8.958	21.135	0.9795
	400	87.75	7.599	29.895	0.9889
6	200	32.14	6.816	2.402	0.9646
	300	47.45	7.553	4.803	0.9857
	400	61.90	10.985	22.449	0.9881
Adsorbent (g/l)	Dye concentration (mg/l)	Pseudo second order			
		$K_2 \times10^{-3}$ g/mg (min)	q_e (cal) (mg/g)	h	r^2
2	200	2.4124	95.238	21.881	0.9978
	300	1.2391	128.205	20.366	0.9934
	400	0.8268	169.49	23.752	0.9939
4	200	18.2130	48.543	42.918	0.9999
	300	7.5870	72.463	39.840	0.9999
	400	3.2391	95.238	31.055	0.9996
6	200	55.4412	32.573	85.470	0.9999
	300	37.3351	47.846	85.470	0.9999
	400	9.7343	64.102	40.000	0.9999

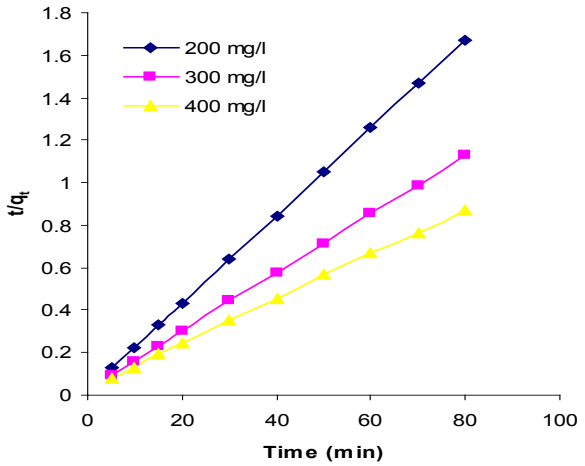

Fig. 6. Second order kinetic plots for the removal of Safranine at different initial dye concentrations; adsorbent dose 4 g/l, pH 8.

200, 300, 400 mg/l. The experimental data showed a good compliance with the pseudo second order equation and correlation coefficients (r^2) for linear plots are higher than 0.9939 (Table 3) for all the experimental data. Also, the calculated qe values agree with the experimental data. This indicates that adsorption system belongs to the pseudo second order model, based on the assumption that the rate limiting step may have chemisorptions, provides best correlation of the data for GNS adsorbent. It has been observed that rate constants for second order model decreased with an increase in initial dye concentration and increases with increase in adsorbent dose (Table 3). The initial adsorption rate h was found to be decreases from 42.918 to 31.055 mg/g min as dye concentration increases from 200 to 400 mg/l for adsorbent dose of 4 g/l. The h values are increases from 21.88 to 85.47 mg/g min as adsorbent dose increases from 2 to 6 g/l for 200 mg/l dye concentration (Table 3).

3.5.3. The Elovich equation

The Elovich equation is given as follows [21]:

$$q_t = \frac{1}{\beta}\ln(\alpha\beta) + \ln t\frac{1}{\beta} \quad (3)$$

where α is the initial adsorption rate (mg g^{-1} min^{-1}), β is the desorption constant (g/mg), To simplify Elovich equation, Chien and Clayton assumed $\alpha\beta\ t >> t$ and by applying boundary conditions $q_t = 0$ at $t = 0$ and $q_t = q_t$ at $t = t$ to get Eq. (3), α and β were calculated from intercept and slope of the straight line plot of q_t vs. ln t .It was seen from the data that the value of α and β varied as a function of the initial dye concentration. Thus increasing the initial dye concentration from 200 to 400 mg/l, the value of β decreases from 0.0893 to 0.0402 g/mg for 2 g/l, from 0.3486 to 0.1046 g/mg for 4 g/l and from 1.2645 to 0.2235 g/mg for 6 g/l of the adsorbent dose. As the adsorbent dose increases from 2 to 6 g/l, β value also increases from 0.0893 to 1.2645 g/mg for 200 mg/l of dye solution (Table 4). The initial adsorption rate a decreases from 5.174×10^2 to 1.665×10^2 mg/g min as dye concentration was increased from 200 to 400 mg/l for adsorbent dose of 2 g/l. As adsorbent dose increases from 2 to 6 g/l initial adsorption rate a was increased from 5.174×10^2 to 7.047×10^{15} mg/g min (Table 4).

The comparison of initial adsorption rates h and α (Table 3 and 4) show that as dye concentration increases the values of h and α decreases while as adsorbent dose increases h and α values are increases.

3.5.4. The intraparticle diffusion model

The nature of the rate limiting step in batch system can also be accessed from the properties of the solute and adsorbent. Weber and Morris [22] stated that if intra-particle diffusion is the rate of controlling factor, uptake of the adsorbate varies with the square root of time. Thus rates of adsorption capacity of the adsorbent

Table 4
Adsorption parameters of Safranine onto GNS for Elovich and Intra-particle diffusion models

Adsorbent (g/l)	Dye concentration (mg/l)	Elovich model			Intraparticle diffusion	
		β (g/mg)	α (mg/g min)	r^2	K_p (mg/g/$min^{0.5}$)	r^2
2	200	0.0893	5.174×10^2	0.9766	4.3282	0.9191
	300	0.0575	2.096×10^2	0.9506	6.9001	0.9376
	400	0.0402	1.665×10^2	0.9646	9.8064	0.9426
4	200	0.3486	9.151×10^5	0.8546	1.0416	0.7099
	300	0.1913	6.403×10^4	0.9317	1.9571	0.8236
	400	0.1046	2.052×10^3	0.9628	3.6339	0.8731
6	200	1.2645	7.047×10^{15}	0.9351	0.2966	0.8285
	300	0.7522	7.557×10^{13}	0.9128	0.4921	0.7876
	400	0.2235	8.968×10^4	0.9281	1.6752	0.8194

as a function of the square root of time [23]. The root time dependence, also known as a Weber–Morris plot may be expressed by Eq. (4).

$$q_t = K_p t^{1/2} + C \quad (4)$$

where K_p is intra-particle diffusion rate constant (mg g^{-1} min$^{-0.5}$). According to Eq. (4), a plot of q_t vs. $t^{1/2}$ should be straight line with a slope K_p and intercept C, when the adsorption mechanism follows the intra-particle diffusion process. The dependencies of q_t vs. $t^{1/2}$ for different dye concentrations are shown in Fig. 7. As can be seen from Fig. 7, the plots of q_t against $t^{½}$ consist two linear sections with different slopes. A similar multi-linearity has been observed in other systems [24,25]. The multi-linearity indicates that two or more steps occur in adsorption process. The two linear sections in the root time plots were evaluated separately using Eq. (4), and the model parameters of first section are listed in Table 4. The first straight portion is attributed to the macro-pore diffusion (Phase I) and the second linear portion to micro-pore diffusion (Phase II) [26]. In the first section, the diffusion rate parameter varies with the dye concentration. In the second section the diffusion rate does not exhibit a distinct dependence on the dye concentration.

3.6. Adsorption isotherms

To optimize the design of an adsorption system for the adsorption of adsorbate, it is important to establish the most appropriate correlation for equilibrium curves. The Freundlich and Langmuir isotherm equations have been used to describe the equilibrium characteristic of adsorption.

3.6.1. Freundlich isotherm

The Freundlich isotherm equation is derived by assuming a heterogeneous surface with a non-uniform distribution of heat of adsorption over the surface. The logarithmic form of Freundlich isotherm equation is

$$\log q_e = \log K_f + \frac{1}{n}\log c_e \quad (5)$$

where K_f is the quantity of dye adsorbed in mg/g adsorbent for unit concentration of dye and $1/n$ is a measure of adsorption density and is heterogeneity factor. K_f and $1/n$ can be determined from linear plot of log q_e vs. log C_e (Fig. 8) are presented in Table 4. The linear plot of log q_e vs. log C_e for 100, 200, 300, 400 mg/l dye concentration shows that adsorption follows the Freundlich isotherm. The correlation coefficients (r^2) of the graph are $r^2 > 0.9118$ which indicates the validity of isotherm (Table 5).

High value of K_f shows easy uptake of the dye heterogeneity becomes more prevalent on $1/n$ gets closer to zero. For n = 1 partition between the two phases is independent of the concentration. Value for $1/n$ below 1 indicates a normal Freundlich isotherm; while that above 1 is indicate for co-operative sorption.

3.6.2. Langmuir isotherm

The linear equation of Langmuir is represented as follows [27]. The basic assumption is that the sorption takes place at specific homogenous sites within the adsorbent.

$$(C_e / q_e) = (1/ab) + (C_e / a) \quad (6)$$

where the constant a signifies the adsorption capacity (mg/g) and b is related to energy of adsorption (l/mg). The linear plot of C_e/q_e vs. C_e shows that adsorption follows Langmuir isotherm (Fig. 9). Values of a and b were calculated from the slope and intercept of the linear plots and are presented in Table 5. The applicability of the Langmuir isotherm suggests the monolayer coverage of the dye on the surface of GNS. The essential characteristics of

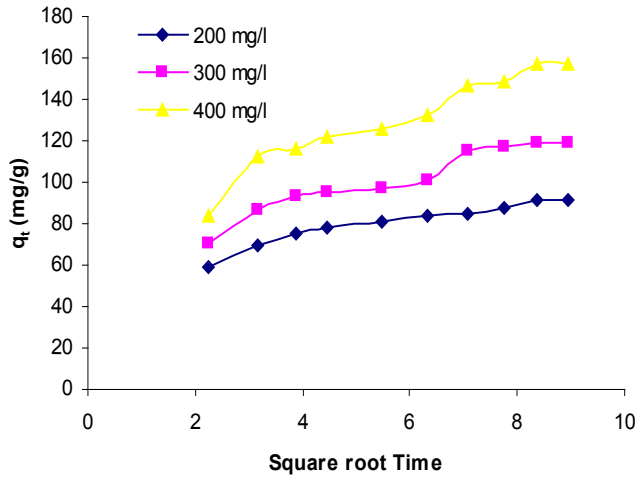

Fig. 7. Weber–Morris plot for adsorption of Safranine by GNS.

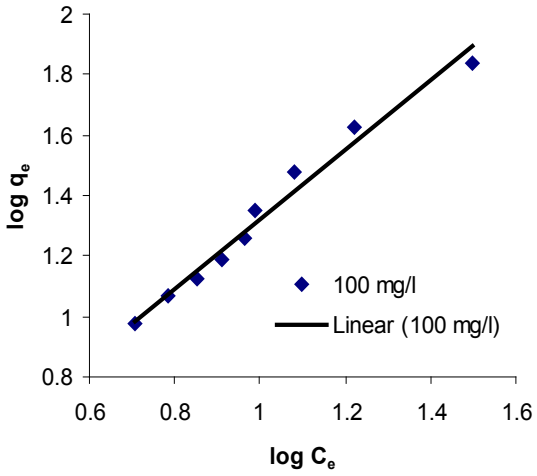

Fig. 8. Freundlich plot for adsorption of Safranine by GNS.

Table 5
Freundlich and Langmuir isotherm constants for adsorption of Safranine on GNS for different dye concentration and adsorbent dose of 1 to 12 g/l at pH = 8, contact time 40 min

Dye concentration (mg/l)	Freundlich coefficient				Langmuir coefficient			
	K_f(l/g)	n	1/n	r^2	a (mg/g)	b (l/mg)	R_L	r^2
100	1.3396	0.8331	1.2002	0.9436	172.413	0.0209	0.3236	0.9948
200	1.4242	0.9827	1.0176	0.9268	114.942	0.0287	0.1480	0.9949
300	1.7918	1.1266	0.8876	0.9275	90.090	0.0465	0.0667	0.9956
400	1.8142	1.1926	0.8385	0.9118	114.942	0.0156	0.1380	0.9898

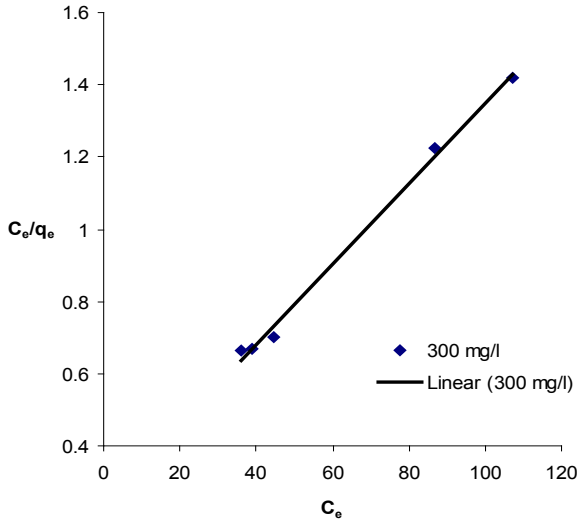

Fig. 9. Langmuir plot for adsorption of Safranine by GNS.

Langmuir isotherm can be expressed by dimensionless separation factor R_L [28].

$$\text{Separation factor} \quad R_L = 1/(1+bC_i) \tag{7}$$

where b is the Langmuir constant related to the affinity of the bonding sites, C_i is the initial dye concentration (mg/l) and R_L value of separation factor indicates the nature of adsorption process. In the present study the value of R_L computed are < 1, indicating that the adsorption process is favorable.

The Freundlich and Langmuir coefficients are shown in Table 5, both the isotherms were found to fit well to the experimental data, the Langmuir isotherm fits well with the experimental data r^2 = 0.9898–0.9956, where as slight low correlation coefficient (r^2 = 0.9118–0.9436) shows slight poor agreement between the Freundlich isotherm and experimental data.

4. Conclusion

The adsorption of Safranine from aqueous solution onto GNS was studied. It was observed that GNS, an agro-based waste biomaterial, can be used as an adsorbent for removal of Safranine from aqueous solution. Adsorption tests were carried out as a function of contact time, pH, adsorbent doses and initial dye concentrations. The amount of dye uptake (mg/g) was found to increase with an increase in solution dye concentration and contact time while found to decrease with adsorbent dosage. The adsorption kinetics can be described by the pseudo second order reaction model. The equilibrium between the adsorbate in the solution and on the adsorbent surface was practically achieved in 40 min. Equilibrium adsorption data for Safranine on GNS were best represented by Langmuir isotherm, the adsorption capacity a = 172.4 mg/g was observed at 100 mg/l dye concentration in optimized conditions. Thus GNS showed excellent adsorptive characteristics for the removal of Safranine from aqueous solution.

Acknowledgments

The authors are gratefully acknowledged to the Head, Centre for Nanomaterials and Quantum Systems, Department of Physics, University of Pune for SEM, XRD and EDX analysis. Authors are also thankful to Principal, GTP College Nandurbar for providing necessary laboratory facilities.

References

[1] M. Valix, W.H. Chaung and G. McKay, Preparation of activated carbon using low temperature carbonization and physical activation of high ash raw bagasse for acid dye adsorption, Chemosphere, 56 (2004) 493–501.
[2] B.H. Hammed, Removal of cationic dye from aqueous solution using jack fruit peel as non-conventional low cost adsorbent, J. Hazard. Mater., 162 (2009) 344–350.
[3] M. Arami, N.Y. Limaee and N.M. Mahmoodi, Evaluation of the adsorption kinetics and equilibrium for the potential removal of acid dyes using a biosorbent, Chem. Eng. J., 139 (2008) 2–10.
[4] G. McKay, H.S. Blair and J.R. Gardner, Rate studies for the adsorption of dye stuff on chitin, J. Colloid Interf. Sci., 95 (1983) 108.
[5] D. Mehmet, O. Ysemin and A. Viahir, Adsorption kinetics and mechanism of cationic methyl violet and methylene blue dyes onto sepiolite, Dyes Pigments, 75(3) (2007) 701–713.
[6] S.V. Mane, I.D. Mall and V.C. Shrivastava, Use of bagasse fly ash as an adsorbent for the removal of brilliant green dye from

aqueous solution, Dyes Pigments, 73 (2007) 269–278.
[7] G. Annadurai, R. Juang and D. Lee, Use of cellulose based wastes for adsorption of dyes from aqueous solutions, J. Hazard. Mater., B92 (2002) 263–264.
[8] C. Sathy and P.N. Pramada, Rice husk ash as an adsorbent for methylene blue-effect of ashing temperature, Adsorption, 12 (2006) 27–43.
[9] T. Robinson, B. Chandran and P. Nigam, Removal of dyes from Synthetic textile dye efficient by bio-sorption on apple pumice and wheat straw, Wat. Res. 36 (2001) 2824–2830.
[10] O. Tune, H. Tanaci and Z. Aksu, Potential use of cotton plant wastes for the removal of remazoal black-B reactive dye, J. Hazard. Mater., 163 (2009) 187–198.
[11] M.M. Nassar, M.F. Hamoda and G.H. Radwan, Adsorption equilibrium of basic dye stuff onto palm fruit bune particle, Wat. Sci. Technol., 32 (1995) 27–32.
[12] N. Barka, A. Assabbane, A. Naunah, L. Laanab and Y.A. Ichou, Removal of textile dyes from aqueous solutions by natural phosphate as a new adsorbent, Desalination, 235 (2009) 264–275.
[13] Z. Al-Quodah, Adsorption of dyes using shale oil ash, Wat. Res., 34(17) (2000) 4295–4303.
[14] J. Pedro-Silva, S. Sousa, J. Rodrigues, H. Antunes, J.J. Porter and I. Gocalves, Adsorption of acid orange 7 dye in aqueous solutions by spent brewery grains, Separ. Purif. Technol., 40 (2004) 309–315.
[15] K.G. Bhattacharyya and A. Sharma, Kinetics and thermodynamics of methylene blue adsorption on Neem (*Azadirachta indica*) leaf powder, Dyes Pigments, 65 (2005) 51–59.
[16] M. Dogan and M. Alkane, Adsorption kinetics of methyl violet onto perlite, Chemosphere, 17 (2003) 505–528.
[17] B.S. Inbraj and N. Sulochana, Basic dye adsorption on a low cost carbonaceous sorbent- kinetic and equilibrium studies, Indian J. Technol., 9 (2002) 201–208.
[18] P.K. Malik, Use of activated carbons prepared from sawdust and rise husk for adsorption of acid dyes: a case study of acid yellow 36, Dyes Pigments, 56 (2003) 239–249.
[19] M.A. Raut, M.J. Iqbal, I. Ellahi and S.N. Hasany, Kinetic and thermodynamic aspects of ytterbium adsorption on sand, Adsorpt. Sci. Technol., 13(2) (1996) 97–104.
[20] Y.S. Ho and G. McKay, Pseudo second order model for sorption processes, Process Biochem., 34 (1999) 451–465.
[21] G. McKay, Y.S. Ho and J.C.Y. Ng, Biosorption of copper from wastewater: A review, Separ. Methods, 28 (1999) 87–125.
[22] W.J. Weber and J.C. Morris, Kinetics of adsorption on carbon from solution, J. Sanit. Eng. Div. ASCE, 89 (SA2) (1963) 31–59.
[23] Y.S. Ho and G. McKay, Sorption of dyes and copper ions onto biosorbents, Process Biochem., 38(7) (2003) 1047–1061.
[24] Q. Sun and L. Yang, The adsorptions of basic dyes form aqueous solution on modified beat -resin particle, Wat. Res., 37(7) (2003) 1535–1544.
[25] Y. Xue, H. Hou and S. Zhu, Adsorption removal of reactive dyes from aqueous solution by modified basic oxygen furnace slag: Isotherm and kinetic study, Chem. Eng. J., 147 (2009) 272–279.
[26] S.J. Allen, G. McKay and K.Y.H. Khader, Intraparticle diffusion of a basic dye during adsorption onto sphagnum peat, Environ. Pollut., 56 (1989) 39.
[27] A. Aziz, M.S. Ouali, E.H. Elandaloussi, L.C.D. Menorval and M. Lindheimer, Chemically modified olive stone a low cost sorbent for heavy metals and basic dyes removal from aqueous solutions, J. Hazard. Mater., 163 (2009) 441–447.
[28] S.B. Wang and L. Huiting, Kinetic modeling and mechanism of dye adsorption on unburned carbon, Dyes Pigments, 72 (2007) 308–314.